Ultrasound in Med. & Biol., Vol. 29, No. 12, pp. 1749–1757, 2003

0301-5629/03/$–see front matter

ELSEVIER

doi:10.1016/S0301-5629(03)01051-2

● *Original Contribution*

A NEWTONIAN RHEOLOGICAL MODEL FOR THE INTERFACE OF MICROBUBBLE CONTRAST AGENTS

DHIMAN CHATTERJEE and KAUSIK SARKAR
Department of Mechanical Engineering, University of Delaware, Newark, DE, USA

(*Received* 24 *January* 2003; *revised* 11 *June* 2003; *in final form* 15 *July* 2003)

Abstract—A quantitative model of the dynamics of an encapsulated microbubble contrast agent will be a valuable tool in contrast ultrasound (US). Such a model must have predictive ability for widely varying frequencies and pressure amplitudes. We have developed a new model for contrast agents, and successfully investigated its applicability for a wide range of operating parameters. The encapsulation is modeled as a complex interface of an infinitesimal thickness. A Newtonian rheology with surface viscosities and interfacial tension is assumed for the interface, and a modified Rayleigh–Plesset equation is derived. The rheological parameters (surface tension and surface dilatational viscosity) for a number of contrast agents (Albunex®, Optison® and Quantison®) are determined by matching the linearized model dynamics with experimentally obtained attenuation data. The model behavior for Optison® (surface tension 0.9 N/m and surface dilatational viscosity 0.08 msP) was investigated in detail. Specifically, we have carried out a detailed interrogation of the model, fitted in the linear regime, for its nonlinear prediction. In contrast to existing models, the new model is found to capture the characteristic subharmonic emission of Optison® observed by Shi et al. (1999). A detailed parametric study of the bubble behavior was executed using the ratio of scattering to attenuation (STAR). It shows that the encapsulation drastically reduces the influence of resonance frequency on scattering cross-section, suggesting possible means of improvement in imaging at off-resonant frequencies. The predictive capability of the present model indicates that it can be used for characterizing different agents and designing new ones. (E-mail: sarkar@me.udel.edu) **© 2003 World Federation for Ultrasound in Medicine & Biology.**

Key Words: **Interfacial rheology, Ultrasound, Contrast agent, Encapsulation, Subharmonic, Optison®.**

INTRODUCTION

Intravenously-introduced encapsulated microbubbles have become an accepted contrast-enhancing agent in diagnostic ultrasound (US) imaging. Bubbles are good contrast agents due to their high scattering cross-sections compared with rigid particles. Micrometer-sized free bubbles, which can pass through capillaries, quickly dissolve due to gas diffusion under high osmotic pressure. Use of an encapsulation (typically protein/lipid/surfactant layer) stabilizes the bubbles against dissolution and increases their shell-life. However, it also reduces agents' echogenicity. To achieve a better design of agents with improved functioning, we need to have a quantitative understanding of the role played by the interface.

Experiments have been performed on various contrast agents to characterize their contrast properties (see, for example, de Jong et al. 1992; de Jong and Hoff 1993; Frinking and de Jong 1998; Shi et al. 1999; Hoff et al. 2000; Morgan et al. 2000 or Soetanto and Chan 2000). The data have been interpreted by creating various models. Most models are based on the relatively well-understood dynamics of a free bubble (Leighton 1994). However, encapsulation remains a challenge with only a few attempts at its detail modeling. Roy et al. (1990) treated the encapsulation as a simple viscous liquid layer, and de Jong and coworkers (de Jong et al. 1992; de Jong and Hoff 1993) assumed it to be a viscoelastic solid. They characterized the shell effects using simple lumped parameters in the free bubble equation. Church (1995) provided a detailed model of contrast agents by treating the layer as an incompressible rubbery material, and derived a Rayleigh–Plesset-type equation. He demonstrated the significance of the surface (shell) parameters by varying them over a wide range. Khismatullin and Nadim (2002) used a similar model for the encapsulation, but also considered the outside liquid to be slightly compressible and viscoelastic. They found that liquid

Address correspondence to: Kausik Sarkar, 126 Spencer Lab, Department of Mechanical Engineering, University of Delaware, Newark, DE 19716 USA. E-mail: sarkar@me.udel.edu

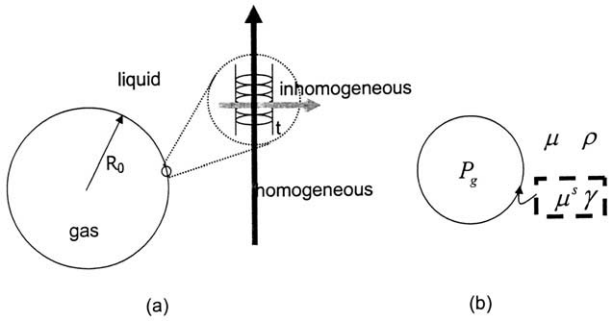

Fig. 1. (a) Schematic of a typical encapsulated bubble; R_0 is the initial bubble radius and t, the thickness of encapsulation. $t << R_0$. (b) The interface model with surface rheology. The symbols are defined in the text.

viscoelasticity and compressibility effects are less important than that of the encapsulation. A purely viscous liquid layer model has been used by Allen et al. (2002) for new therapeutic microbubbles such as MRX-552 (ImaRx Therapeutics, Tucson, AZ). They use the bulk viscosity values of the constituent materials (corn, soy oil or triacetin) of the shell, and successfully compared analytical results with experimental observations.

The continuum modeling of the encapsulation as a layer of finite thickness containing bulk-incompressible material deserves further scrutiny. Biochemical analysis with freeze-etching and electron microscopy delineates the microstructural detail of the shell (Christiansen et al. 1994; Myrset et al. 1996; May et al. 2002). Homogeneous (in all three directions) shell properties and isotropic conditions of these models are not consistent with a shell that is only a few molecules thick (Fig. 1a) and, therefore, highly nonhomogeneous in the thickness direction (Evans and Skalak 1980; Edwards et al. 1991). On the other hand, a completely molecular model, although accurate, is prohibitively expensive to compute, and may not be necessary for determining the acoustic behavior of a bubble. In this paper, we have adopted an interface model (Fig. 1b) for the encapsulation that retains continuum character only in the in-plane direction and, therefore, does not suffer from the above criticism. The interface is assumed to have complex rheological properties due to the presence of adsorbed substances (proteins, lipids and surfactants). Note that such a model has been successfully used for fluid interfaces with adsorbed surfactants and proteins (Graham and Philips 1980), and seems to be more appropriate than the existing models. However, we must admit that the current model, as any other, must ultimately be judged by its capability to predict experimental observations. We have successfully performed such a validation study of the current model.

The predictive validation of the model should be extended to the nonlinear regime critical for harmonic (HI) and subharmonic imaging (SHI). Second harmonic (Chang et al. 1996; Forsberg et al. 1996; Simpson et al. 1999) and subharmonic (Shi et al. 1999; Shankar et al. 1998) emissions have been used to create these imaging modalities. The sub- or superharmonic signal from contrast agents being stronger than those from the surrounding tissue, these modalities provide a higher contrast-to-tissue ratio. Reliability of our model crucially depends on its ability to predict the experimentally observed nonlinear emission.

The main goal of this work was to examine the simplest interfacial rheological model for encapsulation, namely Newtonian, and investigate its validity. The difficulties in determining the interfacial rheological parameters, unlike their bulk counterparts and the interesting findings of this paper, amply justify this simplification in this initial effort. In what follows, we first provide the model and derive the modified equation for encapsulated microbubble dynamics. We used an inverse method to determine the unknown model parameters from experimental data using a linearized form of the equation. Then, we find the model parameters for a number of contrast agents using the data available in the literature. We take Optison® as a case study for investigating our model. Detailed results and discussion of the effects of frequency and amplitude variation on acoustic response are presented.

MATHEMATICAL FORMULATION

Interfacial rheology

The encapsulation of a contrast agent is typically made of very few layers of molecules (Fig. 1a). The structure is not homogeneous in the thickness direction. Neither is it isotropic. The assumption of a homogeneous isotropic layer of finite thickness with constant material properties is clearly inappropriate. However, the encapsulation can be considered as a macroscopic homogeneous continuum in the other two directions. Therefore, one can assume it to be an interface of infinitesimal thickness (Fig. 1b) with complex interface properties "...that represents the effects integrated over the composite molecular structure in the thickness direction..." (page 2 in Evans and Skalak 1980). Such models have been used for biologic membranes as well as fluid interfaces with adsorbed surfactants and proteins (Evans and Skalak 1980; Graham and Philips 1980; Edwards et al. 1991). An interface gives rise to interfacial forces that are modeled by rheology. Here, we have restricted to a Newtonian rheology (*i.e.*, only viscous interfacial stresses). The general form of such an interfacial stress

τ_s, and the jump in traction $[\tau \cdot \mathbf{n}]_{\text{surface}}$ due to it across the surface are given as:

$$\tau_s = \gamma I_s + (\kappa^s - \mu^s)(I_s : D_s)I_s + 2\mu^s D_s, \qquad [\tau \cdot n]_{\text{surface}} = \Delta_s \cdot \tau_s, \quad (1)$$

where γ is the interfacial tension, κ and μ are interfacial dilatational and shear viscosities, I_s, Δ_s and D_s are the surface identity tensor, surface gradient operator and surface strain rate tensor (Edwards et al. 1991).

Encapsulated bubble dynamics

For the liquid-gas system, assuming spherical symmetry (for a micrometer-size bubble in a pressure field of 1 MHz, the radius-to-wavelength ratio is too small, $\sim 10^{-3}$, to produce substantial shape deformation), we have the following (incompressible) mass and momentum equations in the surrounding liquid:

$$\frac{1}{r^2}\frac{\partial}{\partial r}(r^2 v_r) = 0, \quad (2)$$

$$\rho\left(\frac{\partial v_r}{\partial t} + v_r \frac{\partial v_r}{\partial r}\right) = -\frac{\partial p}{\partial r} + \mu\left[\frac{1}{r^2}\frac{\partial}{\partial r}\left(r^2 \frac{\partial v_r}{\partial r}\right) - \frac{2v_r}{r^2}\right], \quad (3)$$

where v_r is the radial component of velocity, ρ the liquid density, p is the pressure and μ is the liquid viscosity. The radial velocity in the liquid is readily obtained from eqn (2) as:

$$v_r = \dot{R}R^2/r^2, \quad (4)$$

where R is the radius of the bubble. Inside the bubble, the gas motion is neglected and a uniform gas pressure $p_i = P_G(t)$ is assumed. Because of spherical symmetry, tangential stresses are zero. Using the Newtonian interfacial stress relation in eqn (1), normal (r-component) stress boundary condition at $r = R$, can be written as:

$$p(r = R, t) = P_G - 4\mu\frac{\dot{R}}{R} - \frac{4\kappa^s\dot{R}}{R^2} - \frac{2\gamma}{R}. \quad (5)$$

We assume a time-varying incident acoustic pressure field:

$$p(\infty, t) = P_o - P_A \sin \omega t, \quad (6)$$

with driving frequency $f(\omega = 2\pi f)$ and amplitude P_A. P_o is the ambient atmospheric pressure. Using continuity and assuming a polytropic behavior with exponent k for the gas ($P_G R^{3k}$ = constant), we integrate the momentum eqn (3), and use boundary condition eqn (5) to arrive at a Rayleigh–Plesset-type equation:

$$\rho\left(R\ddot{R} + \frac{3}{2}\dot{R}^2\right) = P_{G0}\left(\frac{R_0}{R}\right)^{3k} - 4\mu\frac{\dot{R}}{R} - \frac{2\gamma}{R} - \frac{4\kappa^S\dot{R}}{R^2} - P_O + P_A \sin \omega t, \quad (7)$$

where P_{G0}, the initial gas pressure, is given by the initial static balance:

$$P_{GO} = P_G(t = 0) = P_O + \frac{2\gamma}{R}. \quad (8)$$

Equation (7) together with initial conditions, $R(t = 0) = R_0$, and $\dot{R}(t = 0) = 0$ describes the bubble dynamics. The second order differential equation is solved using a stiff solver routine of MATLAB (Math-works Inc, Natick, MA).

Scattering and attenuation cross-sections for nonlinear oscillation

Scattering and attenuation were measured in an acoustic experiment. The model dynamics needs to relate to these measurable quantities. The scattering cross-section (σ_s) is given by:

$$\sigma_s = \frac{W_{\text{scat}}}{I_{\text{inc}}}, \quad (9)$$

where W_{scat} is the scattered power, and I_{inc} is the intensity of the incident acoustic field. These quantities are given by:

$$W_{\text{scat}} = 4\pi\langle r^2 P_s(t)^2\rangle_\tau/(\rho c), \qquad I_{\text{inc}} = \frac{\langle P_A(t)^2\rangle_\tau}{\rho c}, \quad (10)$$

where c is the liquid sonic velocity and $<.>_\tau$ is the average of a quantity over a time interval τ. The acoustic pressure $P_s(t)$ scattered by a bubble is (Brennen 1995):

$$P_s(r, t) = \rho\frac{R}{r}(2\dot{R}^2 + R\ddot{R}). \quad (11)$$

Following Hilgenfeldt et al. (1998), the absorption cross-section σ_a can be defined as:

$$\sigma_a = \frac{W_{\text{dis}}}{I_{\text{inc}}} = \frac{16\pi\rho c\langle\dot{R}^2(\mu R + \kappa^s)\rangle_r}{I_{\text{inc}}}. \quad (12)$$

An ideal contrast agent should produce maximum scattering with minimum absorption. A measure of this

characteristic of a contrast agent is given by Bouakaz et al. (1998) as the ratio of scattering to attenuation (STAR):

$$STAR(f) = \frac{\sigma_s(f)}{\sigma_s(f) + \sigma_a(f)}. \quad (13)$$

Hilgenfeldt et al. (1998) recently showed that the scattered pressure $P_s(t)$ considered here is the active part of the scattered pressure, and the passive part due to density perturbation in the fluid is negligible. We have not considered bubble interactions and directional dependence. The small diameter of these agents compared with the sound wavelength justifies the assumption of isotropy (see Ye 1996 and Allen et al. 2001 for direction dependence). On the other hand, experiments (see, for example, de Jong et al. 1992) showing a linear increase in sound attenuation with bubble concentration suggest absence of any significant bubble-bubble interaction.

Determination of rheological parameters by linearized equation

The bubble dynamics eqn (7) has unknown parameters, interfacial tension γ and dilatational viscosity κ that need to be determined before the model can be put to prediction. We treat the interfacial tension as an unknown—modified from its value for pure gas-liquid interface by the presence of surfactants. Surfactants reduce surface tension by creating a kinetic pressure in the interface (Davies and Rideal 1961). Note that Church (1995), in the finite thickness model of the shell, used two different values of the interfacial tension, one for each interface. We determined the parameters by fitting the model to the attenuation data. Assuming small amplitude of oscillation (*i.e.*, experiments with small forcing), we used a linearized equation of motion for parameter determination, leading to considerable simplicity. The assumption is that these material parameters are independent of the amplitude of oscillation, and the full equation with these parameters can then be used to predict dynamics in the nonlinear regime. We compare the fitted model's nonlinear prediction with experiments in a later section.

The bubble dynamics upon linearization reduces to a damped mass-spring system with well-known resonant frequency and damping term. The resonance frequency that depends on effective "mass" m and the "spring constant" S of the system remains the same as in a free bubble (page 183 in Leighton 1994):

$$\omega_o^2 = \frac{S}{m} = \frac{1}{\rho R_o^2}\left[3\kappa P_o + \frac{2\gamma}{R_0}(3\kappa - 1)\right]. \quad (14)$$

However the damping term δ_{total} will be augmented with an interfacial contribution (Medwin 1977; Hoff et al. 2000)

$$\delta_{\text{total}} = \delta_{\text{liquid}} + \delta_{\text{interface}} + \delta_{\text{radiation}} \quad (15)$$

$$\delta_{\text{liquid}} = \frac{4\mu}{\rho\omega_0 R_0^2}, \quad (16)$$

$$\delta_{\text{interface}} = \frac{4\kappa^s}{\rho\omega_0 R_0^3} \quad (17)$$

$$\delta_{\text{radiation}} = \frac{\omega^2 R_0}{\omega_0 c}, \quad (18)$$

The extinction ($\sigma^{(l)}{}_e$) and scattering ($\sigma^{(l)}{}_s$) for the linearized dynamics are:

$$\sigma^{(l)}{}_e = 4\pi R_0^2 \frac{c\delta_{\text{total}}}{\omega_0 R_0} \frac{\Omega^2}{[(1-\Omega^2)^2 + \Omega^2\delta_{\text{total}}^2]} \quad (19)$$

$$\sigma^{(l)}{}_s = 4\pi R_0^2 \frac{\Omega^4}{[1-\Omega^2)^2 + \Omega^2\delta_{\text{total}}^2]} \quad (20)$$

where Ω is defined as ω/ω_0 (Sarkar and Prosperetti 1994). Therefore, $STAR(f) = \sigma_s(f)/\sigma_e(f)$ (Bouakaz et al. 1998).

The power absorbed and scattered by microbubbles gives rise to attenuation $\alpha(\omega)$ in dB/distance

$$\alpha(\omega) = 10\log_{10}e \int_{a_{\min}}^{a_{\max}} \sigma_e(a;\omega)n(a)da, \quad (21)$$

where $n(a)da$ is the number of bubbles per unit volume with radius in $(a, a+da)$, and $a_{\max(\min)}$ is the maximum (minimum) value of the range of bubble radii. For the case of N bubbles per unit volume of a uniform size, the integral simplifies to $N\sigma_e$. Note that eqn (21) is valid also for nonlinear regime. $\alpha(\omega)$ is a function of the unknown bubble parameters γ and κ. The experimental measurement of attenuation over a range of frequencies $\alpha(\omega)$ is used to define an error $E(\kappa,\gamma)$:

$$E(\kappa^s,\gamma) = \sum_i [\alpha(\omega_i) - \alpha^{\text{meas}}(\omega_i)]^2, \quad (22)$$

The error is minimized to obtain the bubble parameters. MATLAB is used to execute the error minimization.

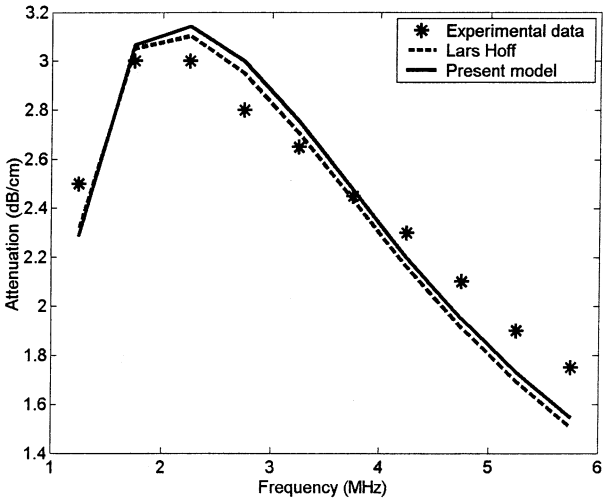

Fig. 2. Determination of the unknown interface (present model) and shell (in case of Lars Hoff's model) parameters corresponding to Optison® bubbles. The experimental data correspond to the work of Shi et al. (1999). Shell thickness is assumed to be 15 nm in Lars Hoff model. G_s = 20.7 MPa and μ_s = 1.7 Pa-s in that model.

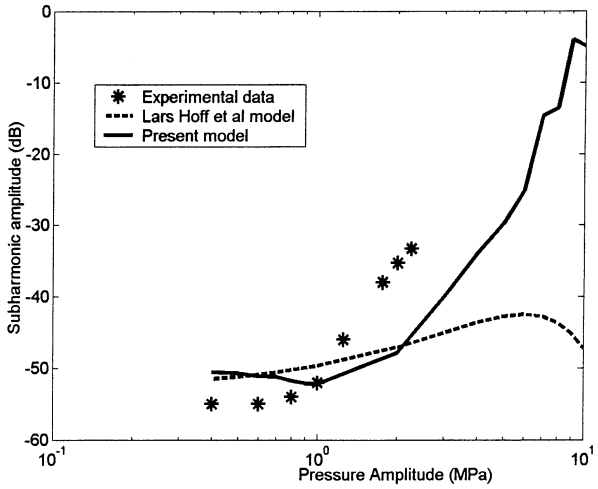

Fig. 3. Variation of subharmonic signal with acoustic pressure amplitude in case of Optison® bubble with a radius of R_0 = 1.5 μm. Driving frequency is 4 MHz and the number of cycles in each pulse is 32. Parameters for Optison® based on present model are described in Table 1 and those for Lars Hoff et al. model is mentioned in caption of Fig. 2.

RESULTS AND DISCUSSION

Characterization of contrast agents: determination of interfacial properties

We applied the method described above to determine dilatational viscosity and interfacial tension for a number of contrast agents. We used attenuation data available in the literature for these contrast agents. We note that the parameter estimation process depends on the attenuation data $\alpha(\omega)$ as well as the bubble size distribution *n(a)*, see eqn (21). Figure 2 shows the observed attenuation data for Optison® (Shi et al. 1999, figure 3 in their paper, data corresponding to 1 min after injection) and the fitted curve using the determined parameters. We used a mean diameter of 3 μm and total number of 6.8×10^8/ml (Shi et al. 1999). In the same figure, we also present the curve for the Church's shell model using the formulation presented by Hoff et al. (2000), equation 6 in their paper. Results for different agents are presented in Table 1. The corresponding references listed in the table contain the attenuation and the radius distribution data for these agents.

Values of dilatational viscosity appear similar to those obtained for other surfactant-laden interfaces (see *e.g.*, Edwards et al. 1991, page 241). However, interfacial tension is an order of magnitude higher than that at the gas-water interface (at an air-water interface γ = 0.072 N/m). Interfacial tension is expected to reduce with the adsorption of surface-active materials. The random motion of the adsorbed surfactant molecules generates a kinetic pressure in the surface, reducing the surface tension. However, in an encapsulation, the molecules are closely packed, forming an elastic membrane with an undeformed equilibrium natural state. Any change in area will lead to an elastic response, a phenomenon commonly known as Gibb's elasticity (see Evans and Skalak 1980, pages 80 and 86). A non-Newtonian viscoelastic rheology might better facilitate the description of the phenomenon. The Newtonian constitutive equation, eqn (1) assumes that the deviatoric part of stress is entirely of viscous origin, having only an isotropic "elastic" term, see also eqn (5), namely the interfacial tension (Kralchevsky and Nagayama (2001). While fitting the data, the elastic effects are lumped into it, generating the unusually high value. Furthermore, Kralchevsky and Nagayama (2001) show that a large curvature, as in the present case of a microbubble, adds an elastic bending effect to the interfacial tension term. The resulting me-

Table 1. Interfacial properties of some commonly used contrast agents

Contrast agent	Dilatational viscosity, κ^s (ms Pa)	Interfacial tension, γ (N/m)
Albunex® (de Jong and Hoff 1993)	0.05	0.78
Optison® (Shi et al. 1999)	0.08	0.90
Quantison® (Frinking and de Jong 1998)	4.24	38.34

chanical interfacial tension is significantly different from its thermodynamic value at a planar interface. Therefore, one could interpret the high value of interfacial tension in the current Newtonian model as the value due to all "elastic" effects (interfacial tension and dilatational elasticity arising from fractional area increase over an unstressed configuration) of the shell.

Model validation for nonlinear emission

To examine the validity of our model, we compared the model prediction with experimental data on nonlinear emission. Note that the model parameters were determined using the linearized equations valid only for small oscillations. However, assuming a Newtonian rheology, the interfacial parameters remain constant in a range of magnitude of oscillation (the parameters may change for too large an oscillation). Figure 3 shows subharmonic emission for Optison® measured by Shi et al. (1999), along with the model prediction. As is evident in the figure, Shi and colleagues found that the process of subharmonic emission involves three stages: occurrence, growth and saturation, as one increases the pressure. Unlike the case of a free bubble, these agents show a distinct occurrence phase marked by little subharmonic emission. Then, it grows with acoustic pressure amplitude and, finally, reaches saturation. Our model predicts this feature with a reasonable agreement with the experimental data. For comparison, we have also included the prediction from Church-Hoff's model (Hoff et al. 2000) using the parameter values indicated in Fig. 2. Although both are matched in the linear regime, only our model satisfactorily compares with experimental observations. This validation encourages us to use our model to predict bubble response under different operating conditions and determine the operating regime in which US contrast agents are likely to have an improved performance.

Dynamics of contrast agent

To further investigate the agent behaviors, we studied the model response with varying diameter, frequency and amplitude. We used interfacial parameters for Optison® listed in Table 1. In Fig. 4, we plot the radius-time curves and their fast Fourier transform (FFTs) for a free bubble and Optison® excited at 2 MHz and 0.1 MPa. The interfacial tension for the free microbubble is 0.072 N/m. The shell considerably damps the oscillations. Figure 5 shows the effect of encapsulation on the functional relation between the resonance frequency and the initial radius of the bubble, see eqn (14). As expected, the increased elasticity due to encapsulation results in an increased resonant frequency. Figure 6 shows the scattering cross-sections with initial bubble radius and driving frequency for small pressure amplitudes (based on linear equations obtained above). From this plot, we see

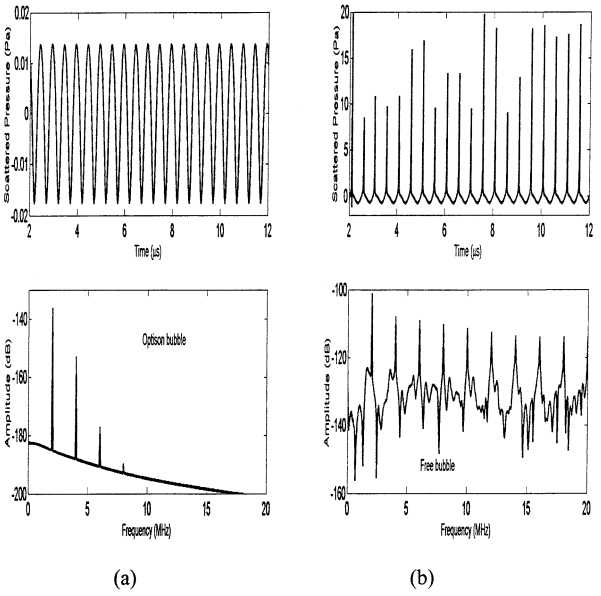

Fig. 4. Time and frequency domain results of scattered pressure due to (a) Optison® and (b) free gas bubbles of initial radius (R_0) 1.5 μm. Driving frequency used is 2 MHz and pressure amplitude is 0.1 MPa.

that the interface elasticity shifts the resonance peak to larger bubble sizes. It also shows a broadening of the resonance peak and a substantial reduction in scattering at resonance due to encapsulation. The deterioration of strong resonance characteristics can explain the observation made by Shi et al. (1999) that, unlike free bubbles,

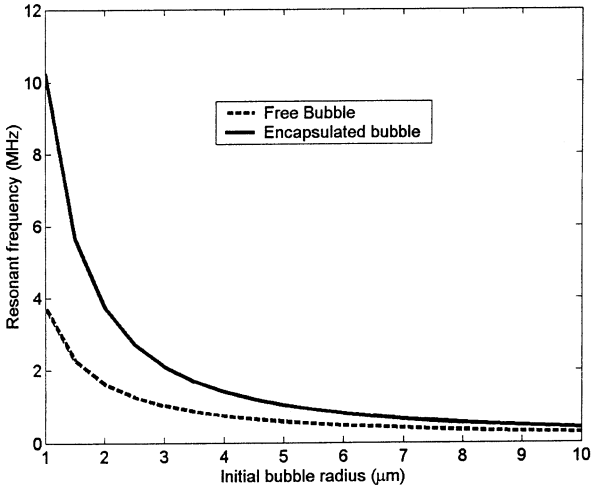

Fig. 5. Effect of initial radius on the resonant frequency. Interfacial properties of Optison® have been chosen to demonstrate the effect of encapsulation.

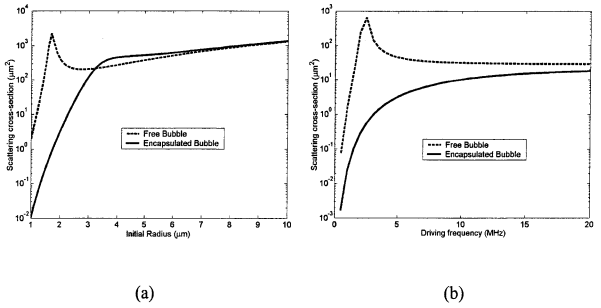

Fig. 6. Effect of (a) initial bubble radius and (b) driving frequency on scattering cross-section for free and encapsulated microbubbles. In (a), driving frequency used is 2 MHz and, in (b), initial bubble radius (R_0) is chosen to be 1.5 μm for both the bubbles.

strong subharmonic emission from Optison® is not obtained with a driving frequency twice the resonant frequency.

Next, we focus on the nonlinear behaviors, critical to harmonic and subharmonic imaging modalities. Figure 7 shows the effect of initial bubble radius on scattering and absorption cross-sections. Note that the linear approximation performs reasonably well for the low pressure level. As a more effective measure of agent performance, STAR is plotted in Fig. 7c. Drop in absorption above the resonant radius $\sim$ 4 μm gives rise to an accelerated increase of STAR with initial radius. Given a driving frequency, variation of initial radius does not result in much improvement in STAR. On the other hand, a higher value (40%) of STAR attained by de Jong and Hoff (1993) at 10 MHz compared to that at resonance is significant.

Figure 8 shows the effect of frequency variation on scattering amplitude for different levels of pressure amplitudes. For low pressure amplitudes, increasing driving frequency leads to an increase in the scattering cross-section. In the typical medical ultrasonic frequency range of 1 to 10 MHz, higher acoustic pressure amplitude results in larger scattering. The effect is more pronounced below 1 MHz, and disappears at frequencies much higher than resonant. At the high-frequency range, the bubble does not get enough time to experience growth and, therefore, the scattering does not increase as much as in the frequency range lower than resonance. The behavior of absorption is similar to that of scattering below 10 MHz. But, above that value, it decreases with frequency and leads to quite high values of STAR.

The model indicates that, operating outside the normal medical range of 1 to 10 MHz, one can obtain better imaging. The mechanical index MI = $P_A/f^{1/2}$ for 1 MPa, 0.6 MHz and 0.6 MPa, 20-MHz pulses are 1.29 and 0.13,

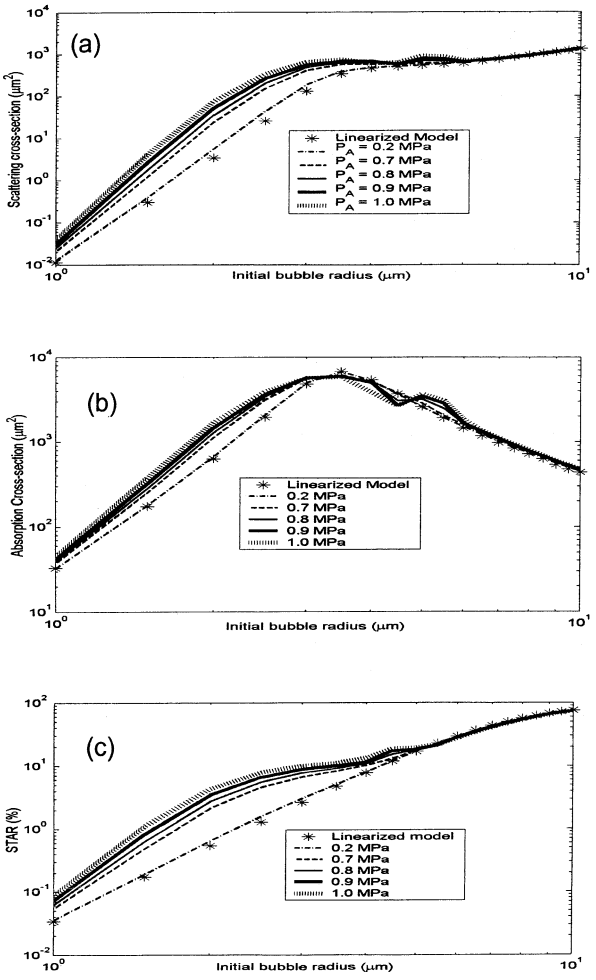

Fig. 7. Effect of initial radius on (a) scattering cross-section, (b) absorption cross-section, and (c) SAR. Also shown in the same figure is the effect of increasing the acoustic pressure amplitude. Driving frequency used is 2 MHz and interfacial properties of Optison® have been used.

respectively; thus, indicating that such insonications are safe (Apfel and Holland 1991). However, we know that a very low frequency leads to poor resolution of the image and too high a value will lead to less depth of penetration. Also, note that the encapsulation may degrade, depending on the value of MI, and our model does not account for that. Further experimental and clinical study is required to investigate the suitability and improvement for these frequencies.

SUMMARY

In this paper, we have reported an interfacial model with intrinsic surface rheology for an encapsulated microbubble used as contrast agent in US imaging. Struc-

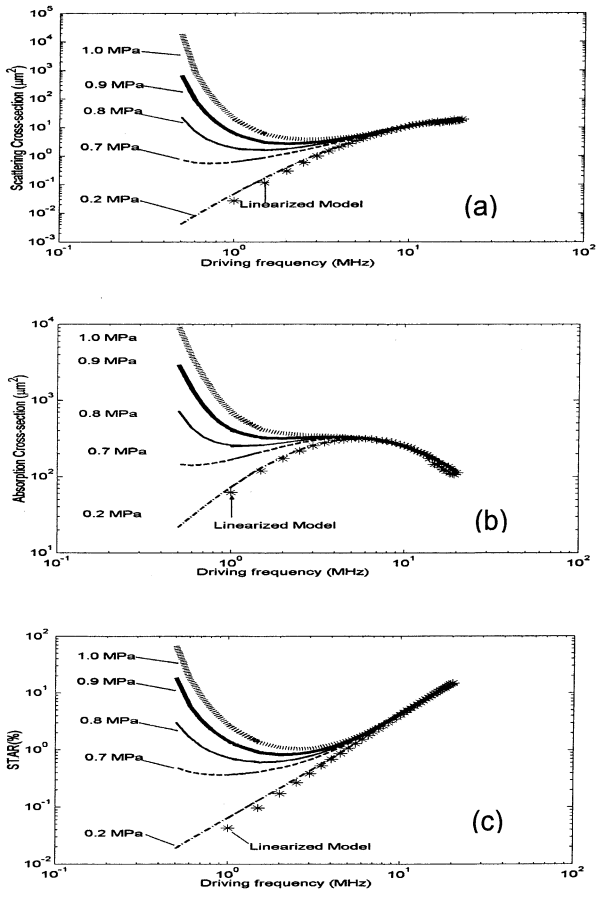

Fig. 8. Effect of driving frequency on (a) scattering cross-section, (b) absorption cross-section, and (c) SAR. Also shown in the same figure is the effect of increasing the acoustic pressure amplitude. Initial bubble radius used is 1.5 μm and interfacial properties of Optison® have been used.

tural detail of the encapsulation provides a rationale for the present model *vis-a-vis* existing ones with a finite shell thickness. Here, we have restricted ourselves to the simplest rheology, namely Newtonian, with two parameters, interfacial tension γ and interfacial dilatational viscosity κ^s. We developed a means to determine the rheological parameters by comparing predictions of a linearized equation with experimentally measured attenuation. A number of contrast agents are characterized with this Newtonian interfacial model. The determined high value of the interfacial tension γ presumably arises from elastic effects. Future work will investigate the suitability of explicit incorporation of viscoelasticity through a non-Newtonian rheology. Our efforts depart from others in the protocol of model validation used here. To validate, we simulated and compared the nonlinear dynamics of Optison® with experiments. In contrast to existing models, the theoretical estimation of subharmonic emission based on the current model compares very well with the experimental results for Optison®. This predictive ability and wider applicability of the current model (the model determined in linear regime predicts nonlinear subharmonic response) compared with its alternatives underscores its importance. Such properties are critical for a reliable characterization tool that can be used toward design of new and improved contrast agents. A parametric study of the behavior of Optison® has been carried out by a numerical solution of the full Rayleigh–Plesset-like bubble equation. The results indicate that the encapsulation drastically reduces the influence of resonance frequency on the backscattering of the contrast agent. It suggests that attempts to exploit the resonant characteristics of a microbubble by carefully choosing the driving frequency may not give the best result. In fact, it is seen that frequencies away from the resonance may yield better results.

Acknowledgments—The authors thank Drs. W.T. Shi and F. Forsberg for the valuable discussions we had with them.

REFERENCES

Allen JS, Kruse DE, Ferrara KW. Shell waves and acoustic scattering from ultrasound contrast agents. IEEE Trans Ultrason Ferroelec Freq Control 2001;48(2):409–418.

Allen JS, May DJ, Ferrara KW. Dynamics of therapeutic ultrasound contrast agents. Ultrasound Med Biol 2002;28(6):805–816.

Apfel RE, Holland CK. Gauging the likelihood of cavitation from short-pulse low-duty cycle of diagnostic ultrasound. Ultrasound Med Biol 1991;17(2):179–185.

Bouakaz A, de Jong N, Cachard C. Standard properties of ultrasound contrast agents. Ultrasound Med Biol 1998;24(3):469–472.

Brennen CE. Cavitation and bubble dynamics. New York: Oxford University Press, 1995:83.

Chang PH, Shung KK, Levene HB. Quantitative measurements of second harmonic Doppler using ultrasound contrast agents. 1996; 22(9):1205–1214.

Christiansen C, Kryvi H, Sontum PC, Skotland T. Physical and biochemical characterization of Albunex, a new ultrasound contrast agent consisting of air-filled albumin microspheres suspended in a solution of human albumin. Biotechnol Appl Biochem 1994;19: 307–320.

Church CC. The effects of an elastic solid surface layer on the radial pulsations of gas bubbles. J Acoust Soc Am 1995;97:1510–1521.

Davies JT, Rideal EK. Interfacial phenomena. New York: Academic Press, 1961.

de Jong N, Hoff L. Ultrasound scattering properties of Albunex microspheres. Ultrasonics 1993;31(3):175–181.

de Jong N, Cornet R, Lancèe CT. Higher harmonics of vibrating gas-filled microspheres. Part one: Simulations. Ultrasonics 1994; 32(6):447–453.

de Jong N, Cornet R, Lancèe CT. Higher harmonics of vibrating gas-filled microspheres. Part two: Measurements. Ultrasonics 1994; 32(6):455–459.

de Jong N, Hoff L, Skotland T, Bom N. Absorption and scatter of encapsulated gas filled microspheres: Theoretical consideration and some measurements. Ultrasonics 1992;30(2):95–103.

Edwards DA, Brenner H, Wasan DT. Interfacial transport processes and rheology. Boston: Butterworth-Heinemann, 1991.

Evans EA, Skalak R. Mechanics and thermodynamics of biomembranes. Boca Raton: CRC Press, 1980.

Forsberg F, Goldberg BB, Liu JB, Merton DA, Rawool NM. On the feasibility of real-time, in vivo harmonic imaging with proteinaceous microspheres. J Ultrasound Med 1996;15:853–860.

Frinking PJA, de Jong N. Acoustic modeling of shell-encapsulated gas bubbles. Ultrasound Med Biol 1998;24(4):523–533.

Graham DE, Phillips MC. Proteins at liquid interfaces, IV. Dilatational properties and V shear properties. J Coll Int Sci 1980;70(3):227 239–250.

Hilgenfeldt S, Lohse D, Zomack M. Response of bubbles to diagnostic ultrasound: A unifying theoretical approach. Eur Phys J B 1998;4: 247–255.

Hoff L, Sontum PC, Hovem JM. Oscillations of polymeric microbubbles: Effect of the encapsulating shell. J Acoust Soc Am 2000; 107(4):2272–2280.

Khismatullin DB, Nadim A. Radial oscillations of encapsulated microbubbles in viscoelastic liquids. Phys Fluids 2002;14(10):3534–3557.

Kralchevsky PA, Nagayama K. Particles at fluids interfaces and membranes. Studies in Interface Science Vol. 10. Amsterdam: Elsevier, 2001:158.

Leighton TG. The acoustic bubble. San Diego, CA: Academic Press, 1994.

May DJ, Allen JS, Ferrara KW. Dynamics and fragmentation of thick-shelled microbubbles. IEEE Trans Ultrason Ferroelec Freq Control 2002;49(10):1400–1410.

Medwin H. Counting bubbles acoustically: A review. Ultrasonics 1977; 15:7–13.

Morgan KE, Allen JS, Dayton PA, et al. Experimental and theoretical evaluation of microbubble behavior: Effect of transmitted phase and bubble size. IEEE Trans Ultrason Ferroelec Freq Control 2000;47(6):1494–1509.

Myrset AH, Nicolaysen H, Toft K, Christiansen C, Skotland T. Structure and organization of albumin molecules forming the shell of air-filled microspheres: Evidence for a monolayer of albumin molecules of multiple orientations stabilizing the enclosed air. Biotechnol Appl Biochem 1996;24:145–153.

Roy RA, Church CC, Calabrese A. Cavitation produced by short pulses of ultrasound. In: Hamilton MF, Blackstock DA, eds. Frontiers of nonlinear acoustics: Proceedings of the 12th ISNA. London, UK: Elsevier, 1990.

Sarkar K, Prosperetti A. Coherent and incoherent scattering by oceanic bubbles. J Acoust Soc Am 1994;96:332–341.

Shankar PM, Krishna PD, Newhouse VL. Advantages of subharmonic over second harmonic backscatter for contrast-to-tissue echo enhancement. Ultrasound Med Biol 1998;24(3):395–399.

Shi WT, Forsberg F, Hall AL, et al. Subharmonic imaging with microbubble contrast agents: Initial results. Ultrasound Imaging 1999;21:79–94.

Simpson DH, Chin CT, Burns PN. Pulse inversion Doppler: A new method for detecting nonlinear echoes from microbubble contrast agents. IEEE Trans Ultrason Ferroelect Freq Control 1999;46(2): 372–382.

Soetanto K, Chan M. Fundamental studies on contrast images from different-sized microbubbles: Analytical and experimental studies. Ultrasound Med Biol 2000;26(1):81–91.

Ye Z. On sound scattering and attenuation of Albunex bubbles. J Acoust Soc Am 1996;100(4):2011–2028.